Earthline Journal of Chemical Sciences
E-ISSN: 2581-9003; CODEN: EJCSB4
Volume 10, Number 2, 2023, Pages 243-266
https://doi.org/10.34198/ejcs.10223.243266

Perturbational Effects of Lithium Cation on Phenytoin Tautomers

Lemi Türker

Department of Chemistry, Middle East Technical University, Üniversiteler, Eskişehir Yolu No: 1, 06800 Çankaya/Ankara, Turkey; e-mail: lturker@gmail.com; lturker@metu.edu.tr

Abstract

Phenytoin is a long-standing, anti-seizure drug used in the treatment of epilepsy, however it has been classified as possibly carcinogenic to humans. It may exhibit 1,3- and 1,5-type proton tautomerism. In the present study, within the constraints of density functional theory at the level of B3LYP/6-31++G(d,p), tautomerism of phenytoin has been investigated. The obtained data collected for vacuum as well as aqueous conditions indicated that the equilibrium concentration of the enol type tautomer should be low. On the other hand, lithium is often referred as an antimaniac drug and used clinically to prevent mood swings in patients with bipolar effective disorder. The present study also considers the mutual interaction of lithium cation and phenytoin at the molecular level. Both the unperturbed and perturbed (by lithium cation) phenytoin tautomers have exothermic heat of formation values and favorable Gibbs free energy of formation values. They are electronically stable. Various quantum chemical data for the unperturbed and perturbed tautomers of phenytoin have been collected and discussed.

1. Introduction

Epilepsy is a serious chronic brain disorder that is characterized by recurrent unprovoked seizures, which in most patients can be successfully treated and controlled with mono- or polytherapy. Antiepileptic drugs (AEDs) are commonly prescribed to control epileptic seizures. Traditional AEDs, carbamazepine (CBZ), phenytoin (PHT) [1-3] and valproate (VPA), are considered to be the first-line treatments for epilepsy in Europe and the United States [3,4].

Phenytoin (5,5-diphenylimidazolidine-2,4-dione) is a long-standing, anti-seizure drug widely used in clinical practice [5]. Phenytoin is a imidazolidine-2,4-dione that consists

Received: July 18, 2023; Accepted: August 12, 2023; Published: August 16, 2023

Keywords and phrases: phenytoin; dilatin; lithium cation; density functional; perturbation.

of hydantoin bearing two phenyl substituents at position-5. It has a role as an anticonvulsant, a teratogenic agent, a drug allergen and a sodium channel blocker. It is functionally related to a hydantoin. Phenytoin binds to the inactivated state of the Na^+ channel to prolong the neuronal refractory period [6].

There are two methods through which phenytoin can be synthesized. Phenytoin synthesis can be achieved by adding base-catalyzed urea to benzyl to produce benzylic acid, from which phenytoin is produced following a rearrangement. This process is called Biltz synthesis of phenytoin [7]. In addition, phenytoin can be produced by oxidation of benzoin with nitric acid to produce the benzyl, after which the procedure is the same as for Biltz synthesis. In this process, almonds may be used as a source of benzaldehyde [8].

Water-soluble phenytoin derivatives have also been synthesized [9]. It should be noted that during decomposition caused by heat, phenytoin typically produces several toxic fumes, including nitrogen oxide, carbon monoxide and carbon dioxide [10].

Phenytoin is metabolized by cytochrome P450 enzyme to 5-(p-hydroxyphenyl)-5-phenylhydantoin (4′-HPPH). Further metabolization to a catechol is possible, and this can extemporaneously oxidize to quinone and semiquinone species [5,11,12].

Phenytoin displays non-linear elimination pharmacokinetics [13]. A result of this non-linearity the elimination half-life differs with plasma concentration.

The mechanism of action of phenytoin in neuropharmacology has been investigated for more than 80 years [14]. Phenytoin is a voltage-gated, sodium channel blocker [15]. It exerts its effect by stabilizing the inactive state of the Na^+ channel and prolonging the neuronal refractory period [16,17].

The mutagenicity of phenytoin and the mutagenicity of its major metabolite, 5-(4-hydroxyphenyl)-5-phenylhydantoin (HPPH), have been tested *in vitro* on different *Salmonella typhimurium* strains (TA1535, TA100, TA1537, TA1538, TA98) using an Ames test [18-20]. Although, from the results of these studies, it was concluded that phenytoin does not have mutagenic properties and experiments in laboratory animals have not provided any evidence of phenytoin carcinogenicity [21-23]; however, in one case the results are inconsistent [24]. Hepatocellular neoplasia in phenytoin-treated rodents have little to no relevance for humans. At present, in the context of epilepsy patients, no link has been found between cancer of the liver and phenytoin [25-27].

Phenytoin, has been widely used since the 1930s as an anticonvulsant in the treatment of epilepsy, however it was classified as possibly carcinogenic to humans [28].

The literature contains some molecular orbital calculations which have been done on phenytoin and phenytoin derivatives [29-33]. Tautomerism can affect the chemical and biological activities of phenytoin. Previously, the tautomerism in phenytoin has been investigated based on the geometries of compounds optimized at the B3LYP/6-31G(d,p) level of theory [34].

The present study considers the tautomerism in phenytoin at B3LYP/6-31++G(d,p) level and also the mutual interaction of lithium cation and phenytoin at the molecular level.

2. Method of Calculations

In the present study, all the initial structure optimizations of the closed-shell structures leading to energy minima have been achieved by using MM2 method then followed by semi empirical PM3 self-consistent fields molecular orbital (SCF MO) method [35,36] at the restricted level [37]. Afterwards, the structure optimizations have been managed within the framework of Hartree-Fock (HF) and finally by using density functional theory (DFT) at the level of B3LYP/6-31++G(d,p) [39,39]. It is worth mentioning that the exchange term of B3LYP consists of hybrid Hartree-Fock and local spin density (LSD) exchange functions with Becke's gradient correlation to LSD exchange [40]. Also note that the correlation term of B3LYP consists of the Vosko, Wilk, Nusair (VWN3) local correlation functional [41] and Lee, Yang, Parr (LYP) correlation correction functional [42]. In the present study, the normal mode analysis for each structure yielded no imaginary frequencies for the $3N$–6 vibrational degrees of freedom, where N is the number of atoms in the system. This search has indicated that the structure of each molecule corresponds to at least a local minimum on the potential energy surface. Furthermore, all the bond lengths have been thoroughly searched in order to find out whether any bond cleavages have occurred or not during the geometry optimization process. All these computations were performed by using SPARTAN 06 [43].

3. Results and Discussion

Phenytoin molecule owes its chemical reactivity to the presence of an imide functional group which may undergo nucleophilic and electrophilic reactions [44,45]. Imide functional group actually can be considered as possessing two embedded lactam moieties. Tautomerism of lactam-lactim (imide-iminol) type should be expected for phytoin at least in theory [45].

Lithium is often referred as an antimaniac drug. Its primary action is preventing mood swings in patients with bipolar effective disorder [2]. Lithium is thought to accelerate the presynaptic destruction of catecholamines. Usually lithium carbonate is used for medication.

Figures 1 and 2 show not only the optimized structures of 1,3- and 1,5-type proton tautomers of phenytoin and their lithium cation composites (perturbed tautomers) but also the direction of their dipole moment vectors. Presence of lithium cation in the vicinity of phenytoin molecule should perturb many properties of the molecule at different extents. The presence of a positive potential field around the cation affects the electron distribution of the neutral molecule (unperturbed tautomer) in such a way that in some cases some electron population is transferred from molecule to the cation. In that case, an intermolecular perturbation can be thought [46].

As seen in Figure 1 direction of the dipole moment vectors varies from one tautomer to another. Whereas in the case of lithium cation composites of phytoin tautomers, the tail of the dipole moment vector originates from somewhere about the imide group which indicates that the cation highly influences the electron distribution of the tautomers. Also orientations of the phenyl groups seem to be affected (some bond lengths might have been affected due to perturbation caused by the presence of lithium cation).

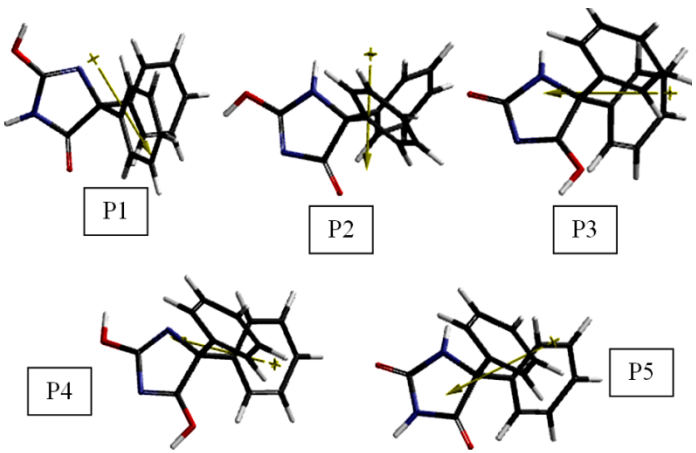

Figure 1. Optimized structures of the tautomers of phenytoin.

From Figure 2, it is also evident that location of the cation exhibits some preference, in some tautomers it prefers the enol vicinity of the lactim form (e.g., P1+Li^+) and in some tautomers the carbonyl moiety of the lactam/lactim form (e.g., P2+Li^+). It should

arise from the variation of electron distribution due to the perturbation has occurred. Meanwhile the phenyl groups arrange their conformations as one tautomer turns into the other one. Approach of the cation should affect the electron distribution of any of the tautomers and as a result, degree of the mutual interaction between the cation and the perturbed molecule dictates the position of the cation around the molecule while the structural optimization occurs.

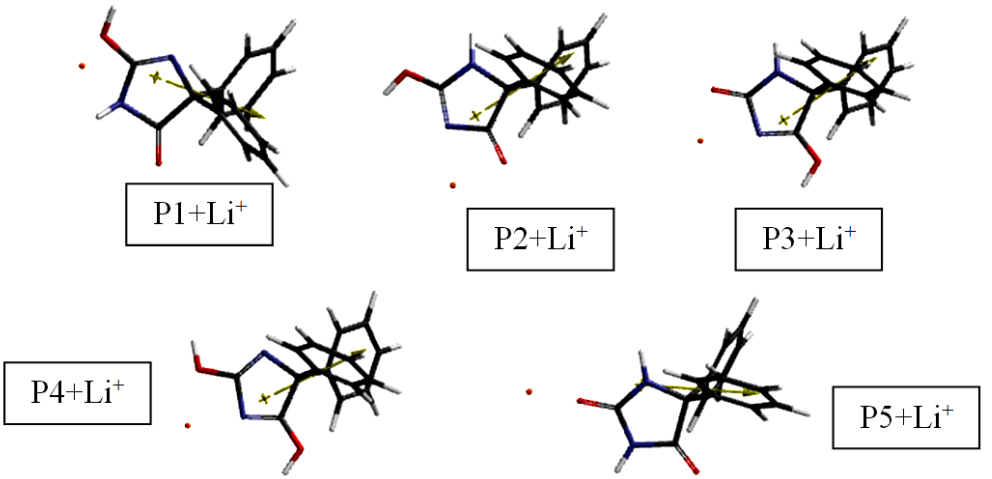

Figure 2. Optimized structures of the tautomers in the presence of lithium cation.

Table 1 lists some thermo chemical values of the tautomers considered. As seen in the table all the tautomers possess exothermic heat of formation and favorable Gibb's energy of formation values at the standard states. The orders of Hº and Gº values are the same in both cases as P5<P1<P3<P2<P4.

Table 1. Some thermo chemical properties of the tautomers considered.

Tautomer	Hº	Sº (J/molº)	Gº
P1	-2201723.549	462.95	-2201861.581
P2	-2201719.527	462.16	-2201857.319
P3	-2201720.624	461.52	-2201858.231
P4	-2201664.490	461.79	-2201802.173
P5	-2201794.585	461.82	-2201932.276

Energies in kJ/mol.

Table 2 contains some thermo chemical properties of the tautomer composites considered. This time the order of both H^o and G^o values are also the same as $P5+Li^+$< $P3+Li^+$< $P2+Li^+$< $P4+Li^+$< $P1+Li^+$. Comparison of the orders for the unperturbed and perturbed systems reveal that the presence of lithium cation shuffles the H^o and G^o values of P1 greatly so that $P1+Li^+$ becomes the last member in the order.

Table 2. Some thermo chemical properties of the tautomer composites considered.

Tautomer	H^o	S^o (J/mol^o)	G^o
$P1+Li^+$	-2220949.048	482.69	-2221092.963
$P2+Li^+$	-2221100.961	481.47	-2221244.514
$P3+Li^+$	-2221103.781	480.64	-2221247.082
$P4+Li^+$	-2220994.385	481.85	-2221138.052
$P5+Li^+$	-2221130.619	482.39	-2221274.445

Energies in kJ/mol.

Tables 3 and 4 list some energies of the tautomers and their lithium cation composites considered, where E, ZPE and E_C stand for the total electronic energy, zero point vibrational energy and the corrected total electronic energy, respectively. The data for E_C values in Table 3 reveal that the stability order is P5>P1>P3>P2>P4. Whereas the stability order in the composite systems (perturbed tautomers) is $P5+Li^+$> $P3+Li^+$> $P2+Li^+$> $P4+Li^+$> $P1+Li^+$ (see Table 4). Again the cation effectively perturbs P1 tautomer hence, electronically $P1+Li^+$ composite is the least stable one in the composite group.

Table 3. Some energies of the tautomers considered.

Tautomer	E	ZPE	E_C
P1	-2202373.26	633.57	-2201739.69
P2	-2202370.25	634.80	-2201735.45
P3	-2202371.92	635.44	-2201736.48
P4	-2202315.40	635.05	-2201680.35
P5	-2202445.71	635.24	-2201810.47

Energies in kJ/mol.

Table 4. Some energies of the tautomer composites considered.

Tautomer	E	ZPE	E_C
P1+Li^+	-2221605.50	637.56	-2220967.94
P2+Li^+	-2221760.91	641.23	-2221119.68
P3+Li^+	-2221764.68	642.39	-2221122.29
P4+Li^+	-2221652.99	639.64	-2221013.35
P5+Li^+	-2221789.76	640.46	-2221149.30

Energies in kJ/mol.

Table 5 shows the aqueous energies and logP values of the tautomers considered. The aqueous energies follow the order of P5< P2< P3< P1< P4. Whereas, the logP order is P5< P3< P2< P1< P4. The log P values are all positive quantities for the unperturbed tautomers. Note that hydrophilic drugs (having low octanol/water partition coefficients) are found primarily in aqueous regions.

Table 5. The aqueous energies and the logP values of the tautomers considered.

Tautomer				
P1	P2	P3	P4	P5
-2202418.96	-2202443.59	-2202429.18	-2202379.94	-2202476.77
1.42	1.26	0.96	2.29	0.55

Energies in kJ/mol.

Figures 3 and 4 show the electrostatic potential (ESP) charges on atoms of the unperturbed and perturbed tautomers, respectively. Note that the ESP charges are obtained by the program based on a numerical method that generates charges that reproduce the electrostatic potential field from the entire wavefunction [43]. Figure 3 indicates that in unperturbed tautomers, the enol oxygen atom (of the lactim form) possesses more negative ESP charge accumulation than the carbonyl oxygen atom (if it exists). In the case of P4, in which only two enol oxygens but not any carbonyl atoms exist, the charges on them are not equal. Structural and electronic variations occurring from tautomer to tautomer considered are to be blamed for the results.

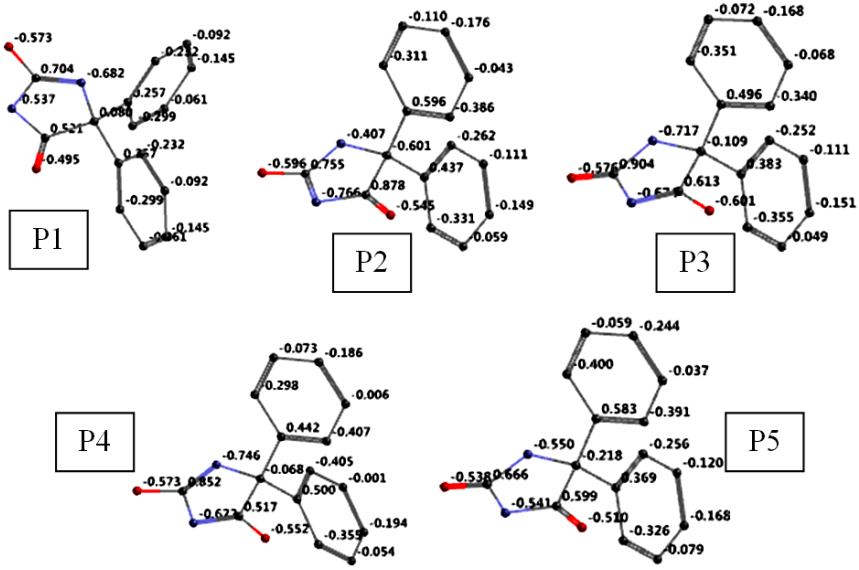

Figure 3. The electrostatic potential (ESP) charges on atoms of the tautomers considered (hydrogens not shown).

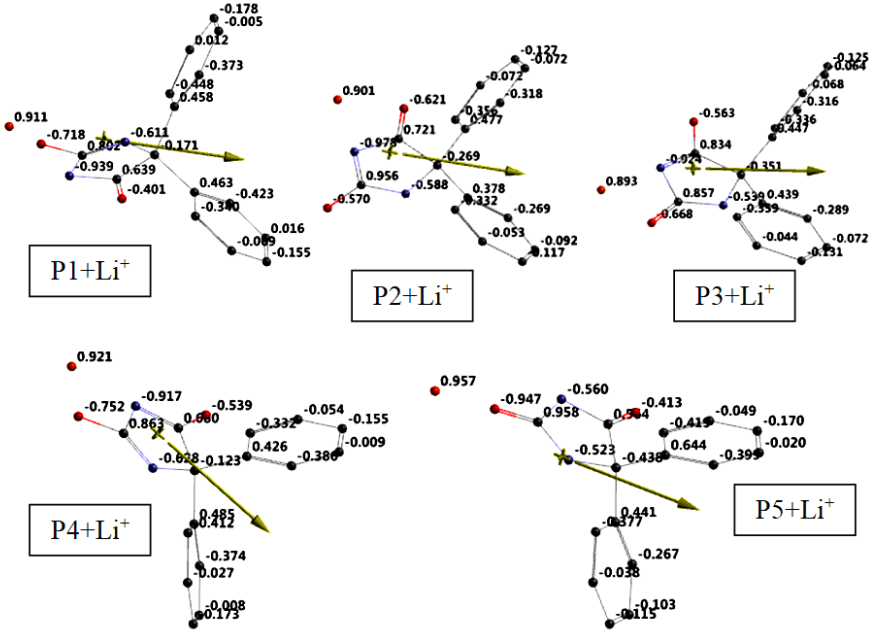

Figure 4. The electrostatic potential (ESP) charges on atoms of the tautomer composites considered (hydrogens not shown).

As for the composites considered, enol oxygen atom of the lactim form possesses more negative charge in the cases of P1+Li^+ and P4+Li^+. In the other tautomers the carbonyl oxygen atom is the more negative one compared to the any existing enol oxygen atom of the lactim form. In all the cases, the positive charge on the lithium cation is less than unity and the order of them is P3+Li^+< P2+Li^+< P1+Li^+< P4+Li^+< P5+Li^+. Consequently, more electron population has been transferred to the lithium cation in the case of P3+Li^+ composite compared to the others.

The ESP maps of the tautomers P1-P5 are shown in Figure 5 where the red and blue colors stand for negative and positive potential regions, respectively. In the figure, note the influence of tautomerism on the potential field over the whole system that has been affected by the location of the tautomeric proton, thus the potential field possesses varying colors from one tautomer to other. In the composites the positive electrostatic potential generated by the cation covers the whole system, thus the maps are all blue without any shade development.

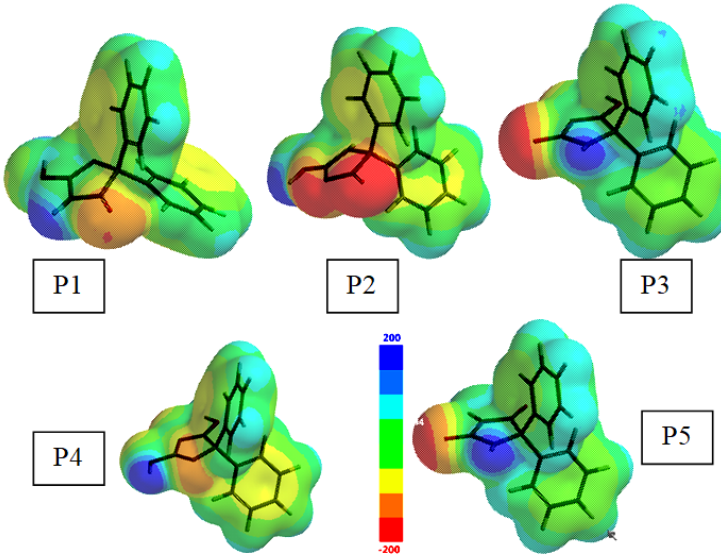

Figure 5. The electrostatic potential maps of the unperturbed tautomers considered

Table 6 contains the dipole moments, polarizabilities and solvation energy values of the tautomers considered. Order of the dipole moments is P4< P1< P5< P2< P3. Note that the resultant dipole moment is the vectorial sum of the bond dipoles in each case. Thus, bond lengths and charges on atoms flanking the bond dictate the individual bond dipole moments.

Order of the solvation energies is P2< P4< P3< P1< P5. The topology of P2 allows a better solvated tautomer among the others whereas P5 having two carbonyl moieties is the least favorably solvated one. Note that P1, P2 and P3 have the same number of carbonyl and enol moieties but their solvation energies are considerably different, which indicates the role of gross and fine topologies of the tautomers on the solvation energies.

Table 6. The dipole moments, polarizabilities and solvation energy values of the unperturbed tautomers considered.

Tautomer	Dipole moment	Polarizability	Solvation Energy
P1	2.53	60.74	-45.70
P2	4.69	60.75	-73.34
P3	5.66	60.73	-57.26
P4	1.48	60.77	-64.54
P5	3.09	60.70	-31.07

Dipole moments in debye units. Polarizabilities in 10^{-30} m^3 units. Energies in kJ/mol.

Table 7 shows the dipole moments and polarizabilities of the tautomer composites considered. The order of dipole moments for the perturbed tautomers is P2+Li^+< P3+Li^+< P4+Li^+< P1+Li^+< P5+Li^+. Recalling that the order of dipole moments for the unperturbed tautomers is P4< P1< P5< P2< P3, the perturbation caused by lithium cation is highly effective and should be due to perturbed charge distribution and bond length/bond angle changes occurred in the presence of lithium cation even though they are not so much.

Table 7. The dipole moments and polarizabilities of the tautomer composites considered.

Tautomer	Dipole moment	Polarizability
P1+Li^+	15.78	61.51
P2+Li^+	10.84	61.30
P3+Li^+	10.94	61.32
P4+Li^+	15.29	61.42
P5+Li^+	18.18	61.35

Dipole moments in debye units. Polarizabilities in 10^{-30} m^3 units.

Tables 8 and 9 include miscellaneous data for the tautomers and their composites considered. Boltzmann distribution values shown in Table 8 reveal that tautomer-5 in vacuum and in aqueous media is the predominant specie which is followed by P1 in the vacuum and by P2 in water. Whereas in the presence of lithium cation, P5 (as P5+Li^+) is followed by P3 (as P3+Li^+) according to Boltzmann distribution values (Table 9). The data reveal that the cation tremendously increases the P3 content (in vacuum the distribution value changes from 1.18586479e-013 to 4.03126533e-005) by means of P3+Li^+ composite. On the other hand, distribution value for P1 is decreased by the cation several folds (from 2.04027174e-013 to 5.26779915e-033).

Table 8. Miscellaneous data for the tautomers considered.

Tautomer	Conformers	HBD	HBA	PSA (Å²)	Boltzmann Dist.	Boltzmann Dist.(aq)
P1	2	1	3	51.258	2.04027174e-013	7.45355064e-011
P2	4	1	3	53.501	6.04205518e-014	1.53721276e-006
P3	4	2	4	53.368	1.18586479e-013	4.59302204e-009
P4	4	2	4	54.030	1.48890655e-023	1.08761255e-017
P5	1	2	4	52.083	1.00000000	0.999998458

HBD: Number of hydrogen bond donor sites. HBA: Number of hydrogen bond acceptor sites.
PSA: Polar surface areas.

Table 9. Miscellaneous data for the tautomer composites considered.

Tautomer	Conformers	HBD	HBA	PSA (Å²)	Boltzmann Dist.
P1+Li^+	4	1	3	51.818	5.26779915e-033
P2+Li^+	2	1	3	51.537	8.83975847e-006
P3+Li^+	2	2	4	50.942	4.03126533e-005
P4+Li^+	4	2	4	51.165	1.09563231e-024
P5+Li^+	1	2	4	49.292	0.999950848

For the abbreviations see Table 8.

The effect of tautomerism on the chemical function descriptors (CFD) of the tautomers are shown in Figure 6. Note that CFDs are attributes given to a molecule in order to characterize or anticipate its chemical behavior. In the figure different colors stand for different descriptors. Note that HBA and HBD mean hydrogen bond acceptor and donors, respectively. The presence of lithium cation does not change the attribution of CFDs except in the case of P2+Li^+ (see Figure 7).

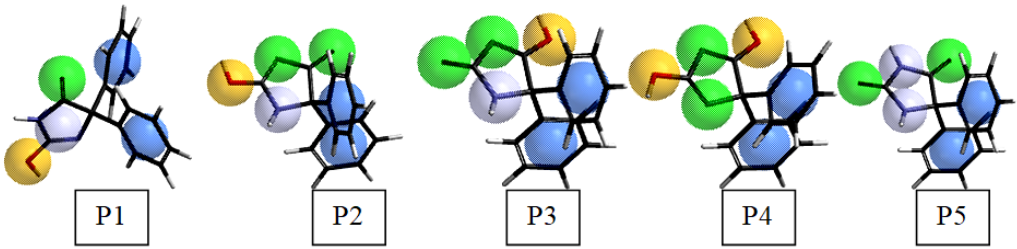

Figure 6. CFDs of the tautomers considered (Green: HBA; Yellow: HBA and HBD; Blue: Hydrophobe; Bluish: HBA, HBD and +ionizable, In P1 Bluish stands for HBA and +ionizable).

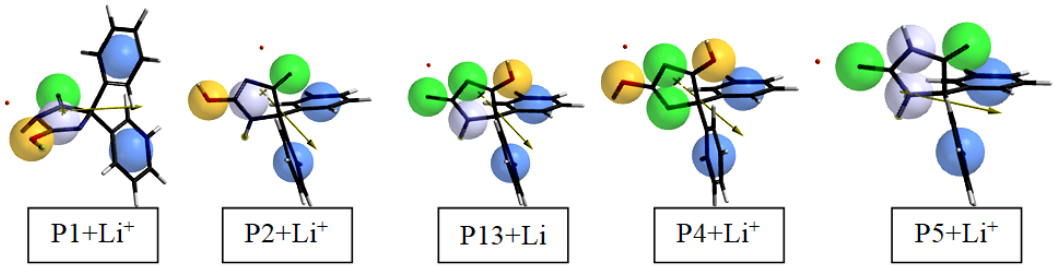

Figure 7. CFDs of the tautomer composites considered. (Green: HBA; Yellow: HBA and HBD; Blue: Hydrophobe; Bluish: HBA, HBD and +ionizable, In P1+Li^+ Bluish stands for HBA and +ionizable).

Figure 8 shows the effect of lithium cation on the distribution of molecular orbital energy levels of the perturbed systems among themselves as well as compared to the unperturbed tautomers. The data reveal that in general both the HOMO and LUMO energy levels are lowered down due to the effect of lithium cation (see Figure 8 and Tables 9 and 10) . So the cation is acting as if an electron withdrawing substituent were attached to the organic molecule, by lowering the frontier molecular orbitals at unequal extends [47]. Moreover, Figure 8 shows that as a result of the perturbation, the energy spacing between the LUMO and NEXTLUMO levels increases. That fact should arise

from the different magnitudes of atomic orbital contributions to LUMO and NEXTLUMO which are affected by the cation. The perturbation also affects the spacing of the inner-lying molecular orbitals so that some nearly degenerate orbitals become distinct ones after the perturbation. Note that those inner-lying molecular orbitals are usually assumed to be effective in contributing to the thermal stability of the molecules.

The HOMO, LUMO energies (ε_{HOMO} and ε_{LUMO}, respectively) and intermolecular orbital energy gap $\Delta\varepsilon$ ($\Delta\varepsilon = \varepsilon_{LUMO}-\varepsilon_{HOMO}$) values of the tautomers and their composites are shown in Tables 9 and 10, respectively. The data in the Table 9 reveal that the orders of the HOMO and LUMO energies are P3< P5< P4< P2< P1 and P3< P4< P5< P2< P1, respectively. Thus, the order of $\Delta\varepsilon$ values for the tautomers, which are one of the contributors to their spectral properties becomes P4< P2< P3< P1< P5.

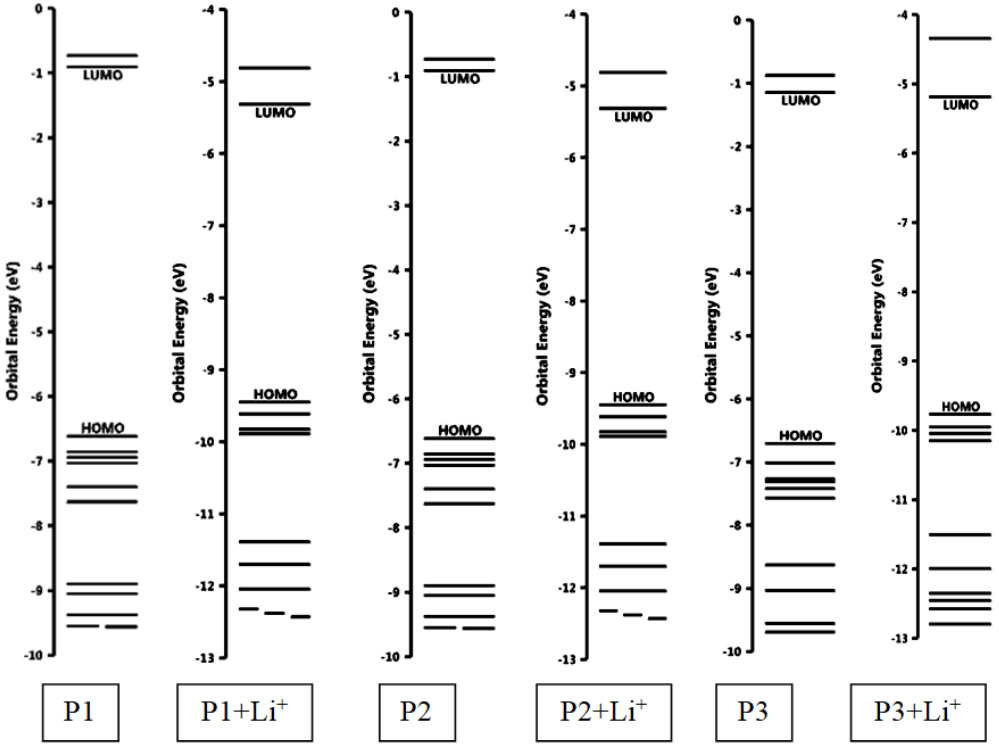

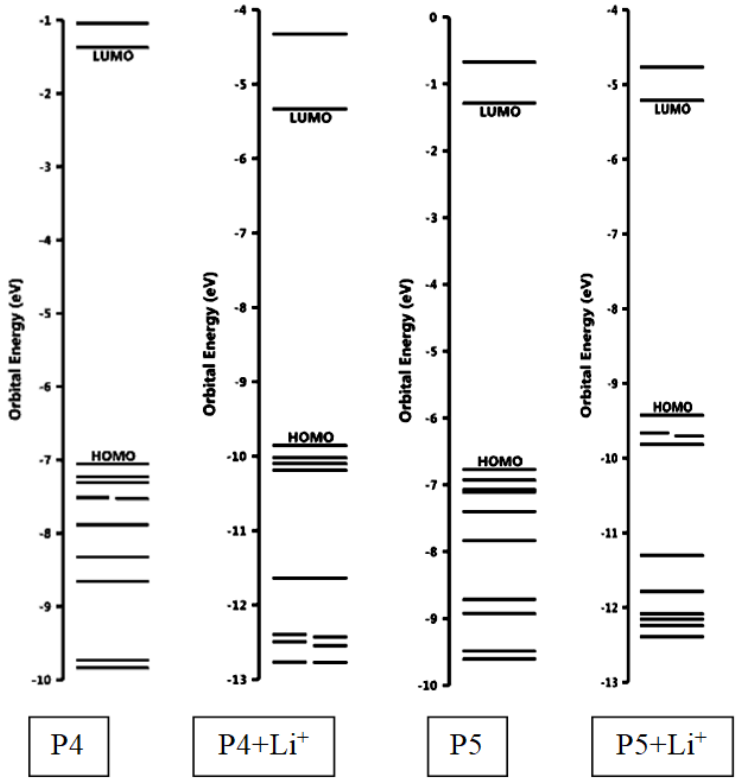

Figure 8. The effect of lithium cation on the distribution of molecular orbital energy levels of the perturbed systems (among themselves as well as compared to the unperturbed tautomers).

Table 9. The HOMO, LUMO energies and Δε values of the tautomers considered.

Tautomer	HOMO	LUMO	Δε
P1	-637.91	-87.22	550.69
P2	-646.73	-110.30	536.43
P3	-680.76	-132.23	548.53
P4	-653.17	-124.03	529.14
P5	-678.41	-112.75	565.66

Energies in kJ/mol.

The data in the Table 10 show that the HOMO energies for the perturbed tautomers follow the order of P3+Li^+< P2+Li^+< P5+Li^+< P1+Li^+< P4+Li^+ whereas the LUMO order is P3+Li^+< P1+Li^+< P4+Li^+< P2+Li^+< P5+Li^+. Consequently, the order of Δε values for the perturbed tautomers becomes P1+Li^+< P4+Li^+< P3+Li^+< P5+Li^+< P2+Li^+. Due to the topology of the five membered ring, the carbonyl group(s) are not equal electronically, thus the lithium cation exerts its perturbational effect utmost on tautomer P3, lowering the HOMO and LUMO energies of P3 resulting the lowest values for P3+Li^+ composite.

Table 10. The HOMO, LUMO energies and Δε values of the perturbed tautomers considered.

Tautomer	HOMO	LUMO	Δε
P1+Li^+	-911.82	-512.70	399.12
P2+Li^+	-942.43	-500.32	442.11
P3+Li^+	-950.77	-514.64	436.13
P4+Li^+	-909.41	-502.76	406.65
P5+Li^+	-914.84	-478.24	436.60

Energies in kJ/mol.

Figure 9 displays the time dependent density functional (TDDFT) UV-VIS spectra of the unperturbed and perturbed tautomers. From the figure one observes that all the

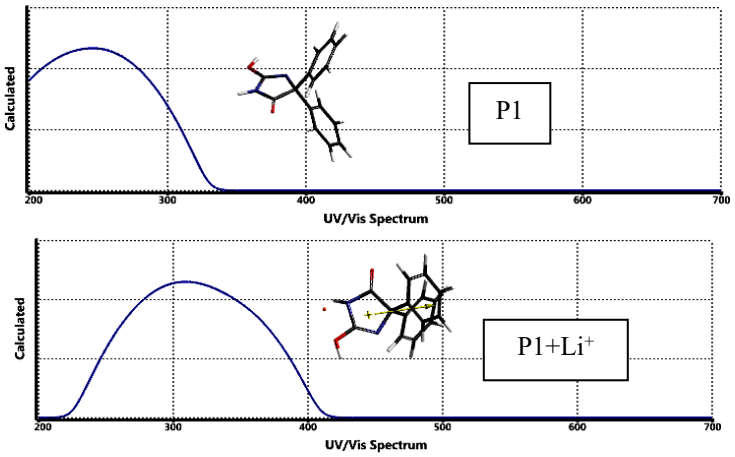

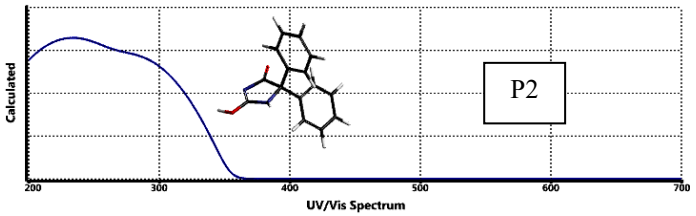
Calculated
200
300
400
500
600
700
UV/Vis Spectrum
P2

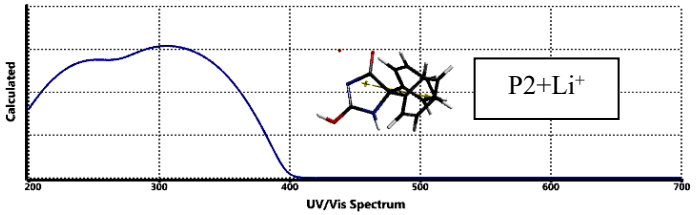
Calculated
200
300
400
500
600
700
UV/Vis Spectrum
P2+Li+

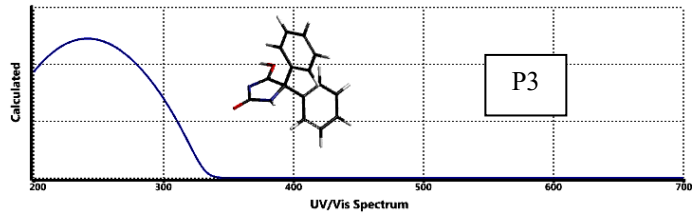
Calculated
200
300
400
500
600
700
UV/Vis Spectrum
P3

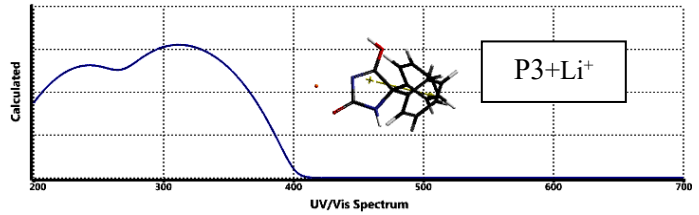
Calculated
200
300
400
500
600
700
UV/Vis Spectrum
P3+Li+

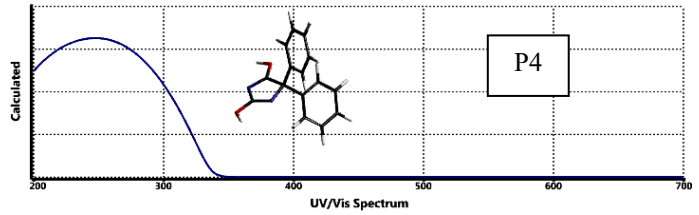
Calculated
200
300
400
500
600
700
UV/Vis Spectrum
P4

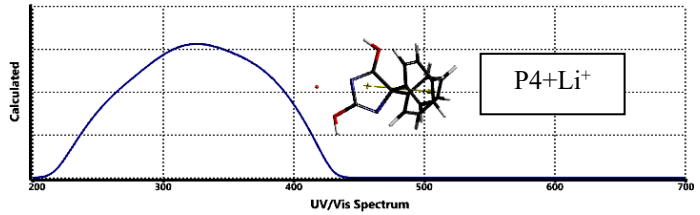
Calculated
200
300
400
500
600
700
UV/Vis Spectrum
P4+Li+

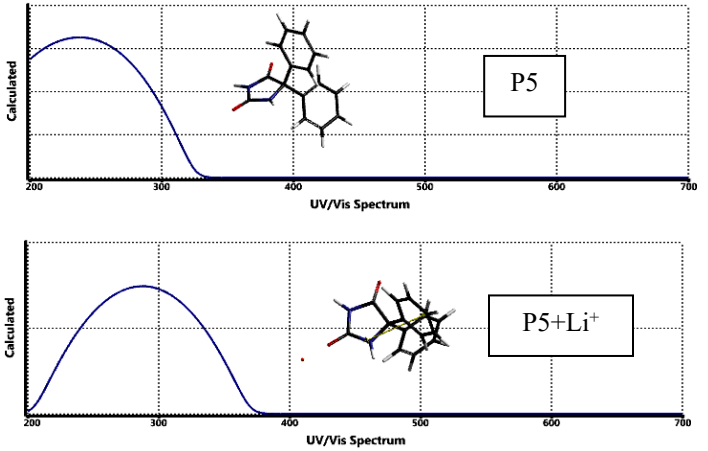

Figure 9. UV-VIS spectra of the unperturbed and perturbed tautomers.

unperturbed tautomers absorb in the UV region. All the perturbed tautomers also absorb in the UV region except P4+Li^+ case which slightly shifts to visible region. However, the rest of the perturbed tautomers also exhibit some bathochromic shift being still in the UV region. In spite of the fact that P2 spectrum exhibits a shoulder, it possesses two absorption peaks in P2+Li^+ case. On the other hand, P3+Li^+ spectrum also has two absorption peaks in contrast to the unperturbed tautomer P3. Note that in the calculated spectra presented, the absorption peaks and their intensities are dictated not only by the HOMO-LUMO transitions but also some other allowed transitions and also their transition moments. Therefore, some spectral shifts or new peaks/shoulders may appear or disappear as the perturbation effect of lithium cation influences the molecular orbitals.

Figure 10 displays the local ionization potential maps of the unperturbed and perturbed tautomers, where conventionally red/reddish regions (if any exists) on the density surface indicate areas from which electron removal is relatively easy, meaning that they are subject to electrophilic attack. In the figure dark blue regions stand for electron poor whereas green/greenish or light blue region relatively electron rich regions.

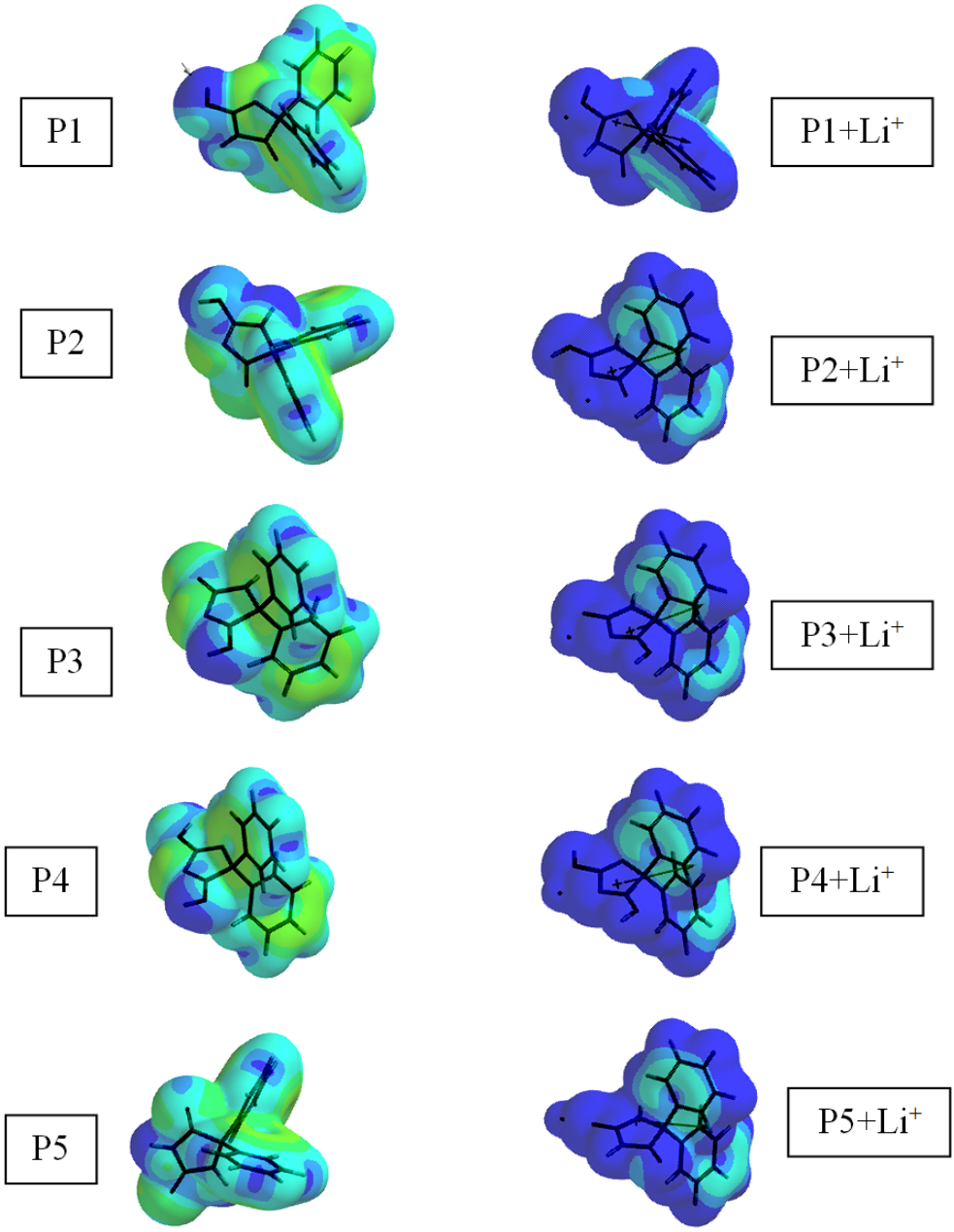

Figure 10. The local ionization potential maps of the unperturbed and perturbed tautomers.

Figure 11 shows the LUMO maps of the of the unperturbed and perturbed tautomers. Note that a LUMO map displays the absolute value of the LUMO on the electron density

surface. The blue color (if any exists) stands for the maximum value of the LUMO and the red colored region, associates with the minimum value.

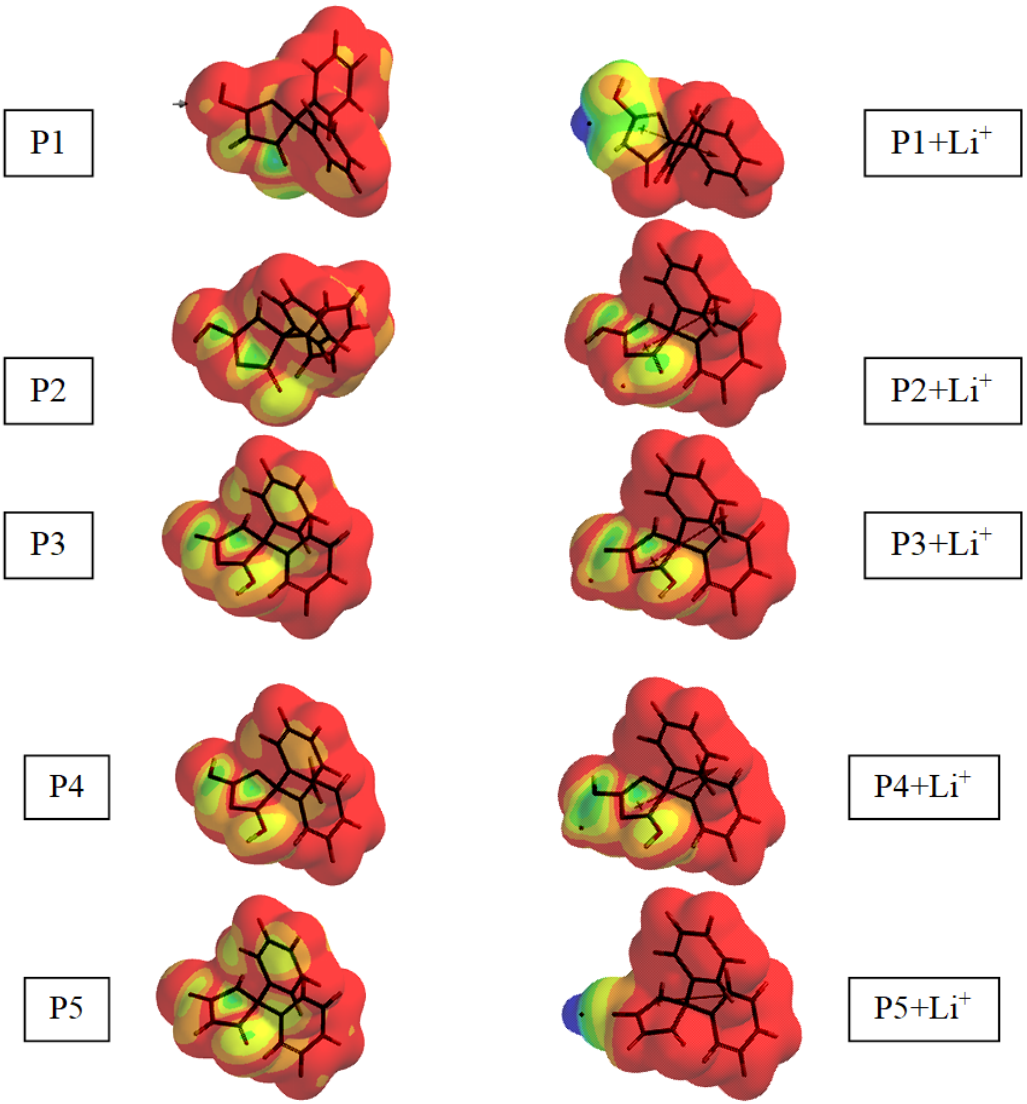

Figure 11. The LUMO maps of the of the unperturbed and perturbed tautomers.

4. Conclusion

The present DFT study at the level of application (B3LYP/6-31++G(d,p) indicates that in vacuum and aqueous conditions the concentrations of lactim type tautomers of the unperturbed as well as the perturbed type phenytoins are low. However, their

concentrations might be increased in polar solvents, because some of them have dipole moments which are higher than that of the imide form. However, the effect of hydrogen-bond donor and acceptor solvents should be rather different. The perturbation caused by lithium cation affects many quantum chemical properties of the tautomers especially the molecular orbital energy levels which are all lowered at unequal extends as compared to the unperturbed ones.

It is a matter of question which is to be thoroughly investigated how those perturbations clinically affect the behavior of patients who are obliged to use both lithium compounds and phenytoin while their treatment period.

References

[1] Windholz, M., & Budavari, S. (Eds.) (1983). *The Merck Index* (10th ed). Rahway, USA: Merck & Co. Inc.

[2] Katzung, B.G. (1984). *Basic and clinical pharmacology*. Lange Medical Pub.

[3] Dreifus, L.S., & Watanabe, Y. (1970). Current status of diphenylhydantoin. *American Heart Journal*, *80*, 709-713. https://doi.org/10.1016/0002-8703(70)90018-9

[4] Zeng, K., Wang, X., Xi, Z., & Yan, Y. (2010). Adverse effects of carbamazepine, phenytoin, valproate and lamotrigine monotherapy in epileptic adult Chinese patients. *Clinical Neurology and Neurosurgery*, *112*(4), 291-295. https://doi.org/10.1016/j.clineuro.2009.12.014

[5] Patocka, J., Wu, Q., Nepovimova, E., & Kuca, K. (2020). Phenytoin - An anti-seizure drug: Overview of its chemistry, pharmacology and toxicology. *Food and Chemical Toxicology*, *142*, 111393. https://doi.org/10.1016/j.fct.2020.111393

[6] Kopsky, D.J., & Hesselink, K.J.M. (2017). Phenytoin in topical formulations augments pain reduction of other topically applied analgesics in the treatment of trigeminal neuralgia. *Journal of Clinical Anesthesia*, *38*, 154-155. https://doi.org/10.1016/j.jclinane.2017.01.040

[7] Safari, J., Naeimi, H., Ghanbari, M.M., & Fini, O.S. (2009). Preparation of phenytoin derivatives under solvent-free conditions using microwave irradiation. *Russian Journal of Organic Chemistry*, *45*(3), 477-479. https://doi.org/10.1134/S1070428009030270

[8] Ashnagar, A., Naseri, G.N., & Amini, M. (2009). Synthesis of 5,5-diphenyl-2,4-imisdazolidinedione (phenytoin) from almond. *International Journal of ChemTech Research*, *1*(1), 47-52.

[9] Bosch, J., Roca, T., Domenech, J., & Suriol, M. (1999). Synthesis of water-soluble

phenytoin prodrugs. *Bioorganic & Medicinal Chemistry Letters*, *9*(13), 1859-1862. https://doi.org/10.1016/S0960-894X(99)00294-2

[10] Lewis, R.J. (2004). *Sr. Sax's Dangerous properties of industrial materials* (eleventh ed.). Wiley-Interscience, Wiley & Sons, Inc., pp. 1302.

[11] Cuttle, L., Munns, A.J., Hogg, N.A., Scott, J.R., Hooper, W.D., Dickinson, R.G., & Gillam, E.M. (2000). Phenytoin metabolism by human cytochrome P450: involvement of P450 3A and 2C forms in secondary metabolism and drug-protein adduct formation. *Drug Metabolism and Disposition*, *28*(8), 945-950.

[12] Ozkaynakci, A., Gulcebi, M.I., Ergec, D., Ulucan, K., Uzan, M., Ozkara, C., Guney, I., & Onat, F.Y. (2015). The effect of polymorphic metabolism enzymes on serum phenytoin level. *Neurological Sciences*, *36*(3), 397-401. https://doi.org/10.1007/s10072-014-1961-8

[13] Browne, T.R., & LeDuc, B. (1995). Phenytoin: chemistry and biotransformation. In R. H. Levy, R. H. Mattson, & B. S. Meldrum (Eds.), *Antiepileptic drugs* (fourth ed., pp. 283-300). Raven Press.

[14] Hesselink, J.M.K. (2017). Phenytoin: a step by step insight into its multiple mechanisms of action—80 years of mechanistic studies in neuropharmacology. *Journal of Neurology*, *264*(9), 2043-2047. https://doi.org/10.1007/s00415-017-8465-4

[15] Hains, B.C., Saab, C.Y., Lo, A.C., & Waxman, S.G. (2004). Sodium channel blockade with phenytoin protects spinal cord axons, enhances axonal conduction, and improves functional motor recovery after contusion SCI. *Experimental Neurology*, *188*(2), 365-377. https://doi.org/10.1016/j.expneurol.2004.04.001

[16] Hesselink, K.J.M., & Kopsky, D.J. (2017). Phenytoin: 80 years young, from epilepsy to breast cancer, a remarkable molecule with multiple modes of action. *Journal of Neurology*, *264*, 1617-1621. https://doi.org/10.1007/s00415-017-8391-5

[17] Hesselink, K.J.M., & Kopsky, D.J. (2017). Phenytoin: neuroprotection or neurotoxicity? *Neurological Sciences*, *38*, 1137-1141. https://doi.org/10.1007/s10072-017-2993-7

[18] Sezzano, P., Raimondi, A., Arboix, M., & Pantarotto, C. (1982). Mutagenicity of diphenylhydantoin and some of its metabolites towards salmonella typhimurium strains. *Mutation Research*, *103*(3-6), 219-228. https://doi.org/10.1016/0165-7992(82)90046-X

[19] Leonard, A., de Meester, C., Fabry, L., de Saint-Georges, L., & Dumont, P. (1984). Lack of mutagenicity of diphenylhydantoin in in vitro short-term tests. *Mutation Research*, *137*(2-3), 79-88. https://doi.org/10.1016/0165-1218(84)90095-8

[20] Riedel, L., & Obe, G. (1984). Mutagenicity of antiepileptic drugs. II. Phenytoin, primidone and phenobarbital. *Mutation Research*, *138*(1), 71-74. https://doi.org/10.1016/0165-1218(84)90087-9

[21] Jang, J.J., Takahashi, M., Furukawa, F., Toyoda, K., Hasegawa, R., Sato, H., & Hayashi, Y. (1987). Long-term in vivo carcinogenicity study of phenytoin (5,5-diphenylhydantoin) in F344 rats. *Food and Chemical Toxicology*, *25*(9), 697-702. https://doi.org/10.1016/0278-6915(87)90103-7

[22] Maeda, T., Sano, N., Togei, K., Shibata, M., Izumi, K., & Otsuka, H. (1988). Lack of carcinogenicity of phenytoin in (C57BL/6 x C3H)F_1 mice. *Journal of Toxicology and Environmental Health*, *24*(1), 111-1119. https://doi.org/10.1080/15287398809531144

[23] Chhabra, R.S., Bucher, J.R., Haseman, J.K., Elwell, M.R., Kurtz, P.J., & Carlton, B.D. (1993). Comparative carcinogenicity of 5,5-diphenylhydantoin with or without perinatal exposure in rats and mice. *Fundamental and Applied Toxicology*, *21*(2), 174-186. https://doi.org/10.1016/0272-0590(93)90234-B

[24] National Toxicology Program. (1993). Toxicology and carcinogenesis studies of 5,5-diphenylhydantoin (CAS No. 57-41-0) (phenytoin) in F344/N rats and B6C3F1 mice (feed studies). National Toxicology Program Technical Report, 404, 1-303. PMID: 12621514.

[25] Dethloff, L.A., Graziano, M.J., Goldenthal, E., Gough, A., & de la Iglesia, F.A. (1996). Perspective on the carcinogenic potential of phenytoin based on rodent tumor bioassays and human epidemiological data. *Human & Experimental Toxicology*, *15*(4), 335-348. https://doi.org/10.1177/096032719601500410

[26] Singh, G., Driever, P.H., & Sander, J.W. (2005). Cancer risk in people with epilepsy: the role of antiepileptic drugs. *Brain*, *128*(Pt 1), 7-17. https://doi.org/10.1093/brain/awh363

[27] Friedman, G.D., Jiang, S.F., Udaltsova, N., Quesenberry Jr., C.P., Chan, J., & Habel, L.A. (2009). Epidemiologic evaluation of pharmaceuticals with limited evidence of carcinogenicity. *International Journal of Cancer*, *125*(9), 2173-2178. https://doi.org/10.1002/ijc.24545

[28] IARC (Some Pharmaceutical Drugs) (1996). Monographs on the evaluation of carcinogenic risks to humans, 66.

[29] Guerrab, W., Lgaz, H., Kansiz, S., Mague, J.T., Dege, N., Ansar, M., Marzouki, R., Taoufik, J., Ali, I.H., Chung, I.M., & Ramli, Y. (2020). Synthesis of a novel phenytoin derivative: Crystal structure, Hirshfeld surface analysis and DFT calculations. *Journal of Molecular Structure*, *1205*, 127630. https://doi.org/10.1016/j.molstruc.2019.127630

[30] Milne, P., Hô, M., & Weaver, D.F. (1999). Interaction of anticonvulsant drugs with metals: a semi-empirical molecular orbital study of phenytoin-zinc(II) complexation. *Journal of Molecular Structure: THEOCHEM*, *492*(1-3), 19-28. https://doi.org/10.1016/S0166-1280(98)00601-0

[31] Serdaroğlu, G., & Ortiz, J.V. (2017). Ab Initio calculations on some antiepileptic drugs such as phenytoin, phenobarbital, ethosuximide and carbamazepine. *Structural Chemistry*, *28*, 957-964. https://doi.org/10.1007/s11224-016-0898-3

[32] Saleh, G.A. (1998). Charge-transfer complexes of barbiturates and phenytoin. *Talanta*, *46*(1), 111-121. https://doi.org/10.1016/S0039-9140(97)00251-8

[33] Luchian, R., Vinţeler, E., Chiş, C., Vasilescu, M., Leopold, N., & Chiş, V. (2015). Molecular structure of phenytoin: NMR, UV-Vis and quantum chemical calculations. *Croation Chemical Acta*, *88*(4), 511-522. https://doi.org/10.5562/cca2767

[34] Sotoodeh, H., Mostafavi, N., & Ebrahimi, A. (1397). Tautomerism in phenytoin: A theoretical study in gas phase. 26th Iranian Seminar on Organic Chemistry, Zabol. https://civilica.com/doc/913561

[35] Stewart, J.J.P. (1989). Optimization of parameters for semi empirical methods I. *Journal of Computational Chemistry*, *10*, 209-220. https://doi.org/10.1002/jcc.540100208

[36] Stewart, J.J.P. (1989). Optimization of parameters for semi empirical methods II. *Journal of Computational Chemistry*, *10*, 221-264. https://doi.org/10.1002/jcc.540100209

[37] Leach, A.R. (1997). *Molecular modeling*. Longman.

[38] Kohn, W., & Sham, L.J. (1965). Self-consistent equations including exchange and correlation effects. *Physical Review*, *140*, A1133-A1138. https://doi.org/10.1103/PhysRev.140.A1133

[39] Parr, R.G., & Yang, W. (1989). *Density functional theory of atoms and molecules*. Oxford University Press.

[40] Becke, A.D. (1988). Density-functional exchange-energy approximation with correct asymptotic behavior. *Physical Review A*, *38*, 3098-3100. https://doi.org/10.1103/PhysRevA.38.3098

[41] Vosko, S.H., Wilk, L., & Nusair, M. (1980). Accurate spin-dependent electron liquid correlation energies for local spin density calculations: a critical analysis. *Canadian Journal of Physics*, *58*, 1200-1211. https://doi.org/10.1139/p80-159

[42] Lee, C., Yang, W., & Parr, R.G. (1988). Development of the Colle-Salvetti correlation energy formula into a functional of the electron density. *Physical Review B*, *37*, 785-789. https://doi.org/10.1103/PhysRevB.37.785

[43] SPARTAN 06 (2006). Wavefunction Inc. Irvine CA, USA.

[44] March, J. (1977). *Advanced organic chemistry*. McGraw-Hill.

[45] Reutov, O. (1970). *Theoretical principles of organic chemistry*. Mir Publishing.

[46] Dewar, M.J.S, & Dougherty, R.C. (1975). *The PMO theory of organic chemistry*. New York: Plenum/Rosetta.

[47] Fleming, I. (1973). *Frontier orbitals and organic reactions*. Wiley.